This is the published version of:

IV International Seminar on ORC Power Systems, ORC2017
13-15 September 2017, Milano, Italy

Experimental observation of non-ideal expanding flows of Siloxane MDM vapor for ORC applications

A. Spinelli[a,*], G. Cammi[a], M. Zocca[b], S. Gallarini[a], F. Cozzi[a], P. Gaetani[a], V. Dossena[a], A. Guardone[b]

[a]*Politecnico di Milano, Energy Department, via Lambruschini 4, 20156 Milano, Italy*
[b]*Politecnico di Milano, Aerospace Science and Technology Department, via La Masa 34, 20156 Milano, Italy*

Abstract

Extensive experimental results characterizing the supersonic expansion of an organic vapor in non-ideal conditions are reported in this paper for the first time. The collected data also allowed the assessment of the accuracy of Computational Fluid Dynamic (CFD) tools employed to predict the non-ideal behavior of such flows, including the consistency of thermodynamic models adopted.

The investigation has been carried out on the converging-diverging nozzle test section of the Test Rig for Organic VApors (TROVA), at the Laboratory of Compressible fluid-dynamics for Renewable Energy Application (CREA) of Politecnico di Milano. Supersonic nozzle flow was chosen as the simplest one of significance for organic Rankine cycle (ORC) turbine channels.

The working fluid under scrutiny is Siloxane MDM, a widely employed compound for high temperature ORCs. MDM vapor expands through the TROVA nozzle at moderate non-ideal conditions in the close proximity of the vapor saturation curve. This is the region where ORC expanders typically operate, thus proving the relevance of the investigation for the ORC community. Indeed, detailed experimental data representative of typical ORC expansions were lacking in the open literature up to date.

Two different nozzle geometries, featuring exit Mach number of 2.0 and 1.5 respectively, were tested, exploring a wide range of thermodynamic inlet conditions and diverse levels of non-ideality, from moderate non-ideal state, indicated by a compressibility factor $Z = Pv/RT \simeq 0.80$, to dilute gas conditions, $Z \geq 0.97$. Maximum operating total pressure and temperature are $P_T \simeq 5$ bar and $T_T \simeq 250$ °C. The nozzle flow is characterized in terms of total pressure, total temperature, static pressure at discrete locations along the nozzle axis, and schlieren imaging. In contrast to the well known case of polytropic ideal gas, the vapor expansion through the nozzle is found to be dependent on the inlet conditions, thus proving the non-ideal character of the flow. This influence is found to be consistent with the one predicted by the quasi-1D theory coupled with simple non-ideal gas models.

Experimental data at the nozzle centerline are compared with those resulting from a two-dimensional viscous CFD calculation carried out using the SU2 software suite and the improved Peng Robinson Stryjek Vera (iPRSV) thermodynamic model. A very good accordance is found, demonstrating the high accuracy of the applied tools.

---

* Corresponding author.
E-mail address: andrea.spinelli@polimi.it

1. Introduction

Nowadays organic Rankine cycle (ORC) power systems represent a cost effective and mature technology for efficient power generation in the range of 1 to 100 MW where thermal power is available at low to medium temperature. This is the case of renewable sources, such as geothermal reservoirs and biomass combustion, and heat recovery from diverse industrial processes (power plants, cement factories) [1,2]. In these power/temperature ranges, ORCs are preferred over steam Rankine cycles due to their relatively high efficiency and the simplicity of cycle configuration.

The expander is certainly a key element of an ORC system, whose efficiency has a significant impact on the whole cycle one. At present, it is mostly constituted by a turbomachine, being the use of volumetric expanders limited to mini or micro-ORCs and to low temperature applications. Current design, optimization and analysis tools for ORC turbo-expanders are based on advanced CFD codes [3–5] embedding state-of-the-art thermodynamic models [6–8], which are required, since the expansion process occurs, for a significant portion, through thermodynamic regions close to the vapor saturation curve and the critical point, where the vapor behavior is far from ideality.

Detailed experimental data for typical turbine channel flows, which are key to assess the accuracy of such tools, are unavailable in open literature up to date. Investigation within industrial turbines is impracticable, due to the limited accessibility of turbine stages and the unavailability of proper instrumentation. The Test Rig for Organic VApors (TROVA) [9–11] was built at the Laboratory of Compressible fluid-dynamics for Renewable Energy Application (CREA) of Politecnico di Milano, with the purpose of filling this gap and, more generally, of carrying out fundamental research in the field of Non-Ideal Compressible Fluid Dynamics (NICFD), namely the branch of fluid-dynamics dealing with compressible flows for which $Pv \neq RT$. Currently, the TROVA test section can be equipped with planar nozzles, designed for different fluids and/or operating conditions; however, it can also accommodate linear blade cascades. A convering-diverging nozzle is indubitably the simplest geometry expanding the vapor from subsonic to supersonic velocity, similarly to ORC turbine channels. Also, the use of a straight axis nozzle entails the possibility of characterizing the flow by resorting to pressure taps and transducers, without the adoption of directional pressure probes, which are still unavailable for such unconventional flows. Moreover, the investigation of the flow within such nozzles or around aerodynamic and bluff bodies located downstream, represent themselves key NICFD experiments.

In this paper, results of an extensive experimental campaign performed on the TROVA nozzle are presented for the first time. Siloxane MDM (octamethyltrisiloxane, $C_8H_{24}O_2Si_3$) was selected as working fluid, since it is widely used in ORC systems and it exhibits a highly non-ideal behavior in the vapor phase [12].

Two different nozzles were designed [13] to obtain a uniform flow at the outlet with Mach number of about 2 and 1.5 respectively, which are typical values for ORC turbine vanes, especially for the initial stages. Each nozzle is tested with variable inlet conditions, from moderate non-ideal to almost ideal gas state (compressibility factor $Z = Pv/RT$ between 0.81 and 0.98). Tests at even higher non-ideal conditions are underway and will be reported in the near future.

The vapor flow is characterized by means of total pressure and total temperature measurements in a settling chamber upstream of the nozzle and by wall static pressure measurements along the nozzle center line. The schlieren technique is also applied to visualize the 2D field of density gradients in the axis direction.

Several tests, carried out in similar conditions, gave comparable results, thus proving test repeatability. For two tests only, results are throughly discussed, underlying non-ideal compressible effects on the expansion process. In particular, the influence of inlet conditions, which is absent in case of the polytropic ideal gas (PIG), is pointed out. The comparison of the flow features with those calculated by modeling MDM vapor as a PIG, showed significant deviation from the ideal behavior, thus proving the importance of accounting for non-ideal effects in the design and performance prediction of ORC turbo-expanders and of any system operating with such unconventional compressible flows. Finally, a comparison with CFD viscous calculations allowed to verify the good accuracy of the SU2 software suite [3,14] in use at the CREA Laboratory for non-ideal compressible flow simulations.

The paper is organized as follows. Section 2 presents the facility and the measurement techniques, while the test procedure is described in section 3. Results are discussed in section 4 and finally, section 5 draws a few conclusions.

2. Experimental facility and measurement techniques

The TROVA facility is a blow-down operation wind tunnel. The working fluid is isochorically heated in a High Pressure Vessel (HPV) up to saturated, superheated, or supercritical conditions at pressure and temperature above the

stagnation conditions at which the nozzle test section is fed. The inlet total pressure P_T is regulated by a fast operating Main Control Valve (MCV). The vapor expands from subsonic to supersonic velocity through the converging-diverging nozzle and it is discharged in a Low Pressure Vessel (LPV). Here the vapor is condensed and pumped back to the HPV by means of a membrane pump. Extensive details about the test rig and its design can be found in [9,11].

2.1. Test section and instrumentation

The plant is conceived to test a wide class of organic fluids at diverse operating conditions; therefore, the TROVA test section can accommodate different, specifically designed nozzles [13]. A planar configuration was preferred, to easily locate an optical access. The adoption of a straight axis nozzle allows to characterize the pressure field at the core, by resorting to the isentropic hypothesis, thus avoiding the use of aerodynamically calibrated pressure probes. This approach does not apply in case the nozzle is highly over-expanded, with shock entering the diverging portion.

Two nozzles were tested. The first one, labelled M2.0, is designed to deliver a uniform flow at the exit with Mach number $M = 2$; each profile presents a backward facing step, machined at the geometrical throat to study the formation of the typical shock structure originating at the trailing edge of supersonic turbine blades, the so-called fishtail shock; details are given in [15,16]. The step non-dimensional height is $h/H = 0.012$, where H is the nozzle semi-height at throat [17,18]. The second nozzle, labelled M1.5, provides a uniform outlet flow at Mach number $M = 1.5$. It is machined with a clean geometry and an increased roughness at the profile surface, to promote the formation of weak waves, whose slope provides a direct measurement of the local Mach number.

Along the axis, 9 pressure taps of 0.3 mm diameter are machined on the rear steel plate, which is mirror polished to perform double passage schlieren; the frontal optical access to the flow is provided by a planar quartz window. Each tap is connected, through a 30 mm long line, to a pressure transducer, which measures wall static pressure P.

Stagnation conditions P_T, T_T are measured in the settling chamber ahead of the test section, using a wall pressure transducer (due to the very low flow velocity) and two K-type thermocouples, whose hot junction of 0.25 mm diameter is located at the chamber axis. Pressure sensors are of piezo-resistive type operating up to 343 °C. Due to their large sensitivity to temperature, they were calibrated both in pressure and in temperature in the range of 1 bar to full scale (FS $\in$ [3.5, 40 bar]) and of 25-300 °C respectively. The K thermocouples were calibrated in the same temperature range (25-300 °C). The final expanded uncertainty is of about 0.07% of the full scale for pressure transducers and of 1 °C for the thermocouples. Concerning the dynamic response of the sensors, the pressure tap trasmission lines exhibit a natural frequency of about 200 Hz, as estimated by applying a viscous model capable to treat complex line-cavity systems [19]. The thermocouple time constant is of about $\tau \simeq 0.25$ s, as estimated using both a theoretical model and the method proposed in [20]. Despite the relatively low response of the thermocouples, no significant lag and distortion of the signal are expected, being the frequency content of the physical signal below 1 Hz for the whole test. In fact, after a dynamic compensation, deviations of the measured signal are found well within the sensor uncertainty.

Schlieren visualization are performed to complement the discrete measurements at the axis with continuous imaging of the density gradient field. The system is of double passage type and is equipped with a high speed CMOS camera, which is digitally triggered to synchronize the schlieren images with the pressure and temperature data. The knife orientation is such that density gradients in the nozzle axis direction are visualized, with compression waves appearing as dark regions and expansion waves as bright ones. Further details on the instrumentation are in [17,18].

3. Test description and operating conditions

Table 1. Total pressure P_T and temperature T_T, total compressibility factor Z_T, adapted expansion ratio β and exit Mach number M_{out} at time $t = 0$.

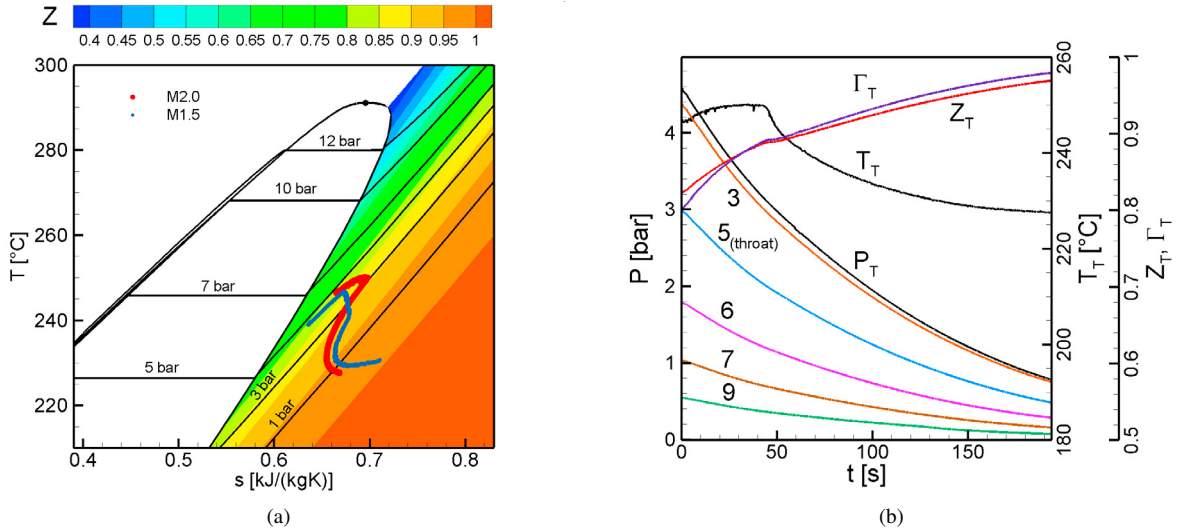| Test	P_T (bar)	T_T (°C)	Z_T	β	M_{out}
M2.0	4.58	246	0.82	8.43	2.03
M1.5	4.59	239	0.81	3.12	1.51

Fig. 1. (a) Explored thermodynamic region for tests M2.0 and M1.5. (b) Time trends of measured P_T, T_T, P and calculated Z_T, Γ_T for test M2.0.

Several tests were performed on the MDM vapor expanding through the two nozzles, M2.0 and M1.5, starting at moderate non-ideal thermodynamic conditions close to the saturation curve. Indeed, the MDM vapor is in a slightly superheated state, at initial total conditions of $P_T \simeq 5$ bar, $T_T \simeq 240$ °C, corresponding to a minimum value of $Z = 0.81$. A very good repeatability has been verified, therefore, only one test for each nozzle is presented here; they are labelled using the nozzle names, M2.0 and M1.5. Early results from experiments at a higher non-ideal states are already available but not reported here for brevity. Full results of this campaign will be available in the near future.

A single test is triggered by the opening of the MCV, which allows the flow to be discharged through the nozzle. The total pressure P_T upstream of the nozzle is not controlled; a 100% opening position of MCV is kept fixed, entailing the opportunity of exploring a wide variety of thermodynamic states during one single run. Indeed, after the opening transient ($\sim$2 s), P_T decreases as the HPV empties; starting from initial moderate non-ideal conditions, the ideal-gas state is approached at the test conclusion. The characteristic time of the nozzle is more than two order of magnitude lower than the one related to the emptying of the HPV [9,11]; thus, a steady state flow can be assumed at a fixed time. Indeed, data are acquired at a high frequency, which is 1 kHz for pressure and temperature mesurements, while the exposure time for schlieren imaging is 1 ms. The test section operates in under-expanded conditions during the entire test; therefore an isentropic flow can be assumed within the large nozzle core, except in the very close proximity of the walls. This hypothesis, verified experimentally for air, is confirmed by CFD for MDM. Table 1 summarizes test conditions at time $t = 0$ s, i.e. at maximum non-ideal state (minimum total compressibility factor Z_T).

Figure 1a shows, in the temperature-specific entropy ($T - s$) diagram, the evolution of the inlet conditions (P_T, T_T) during the test, clarifying that as P_T reduces, Z_T and ideal conditions are approached. Also, the extent of the thermodynamic region explored during a test can be appreciated, as well as and the proximity to the saturation curve. The specific entropy s was calculated as a function of P_T and T_T using the Span-Wagner (SW) model for MDM [6].

4. Experimental results

Results are presented here for the two analysed tests. Firstly, the signals acquired in time are discussed evidencing measured quantities against calculated ones. Then expansion along the nozzle at selected levels of non-ideality are presented in terms of local static-to-total pressure ratio P/P_T, compressibility factor Z and schlieren visualization.

4.1. Time signals

For test M2.0, figure 1b shows the time evolution of the total pressure P_T and temperature T_T, of wall static pressure P, at different locations along the nozzle axis, and of stagnation compressibility factor Z_T and fundamental derivative of gasdynamics Γ_T, both calculated as a function of P_T and T_T by applying the SW model. The test lasts

approximately 195 s, excluding the transient time related to the opening of valve MCV. Static pressure signals are labelled according to the corresponding tap numbers (from 1 to 9) which increase from nozzle inlet to outlet.

Pressure along the nozzle reduces as the vapor flow expands while all pressure values decrease in time due the emptying of the HPV. In contrast, the total temperature T_T does not exhibit a monotonic decreasing trend. This is reasonably due to the non-uniformity of the temperature within the HPV at the test start. A stratification is indeed present in most of the tests performed; a similar evolution is observed for test M1.5, as can be inferred by figure 1a.

The fundamental derivative of gasdynamics [21] is defined as $\Gamma = 1 + \frac{\rho}{c} \left(\frac{\partial c}{\partial \rho} \right)_s$, where c is the speed of sound, ρ is the density and s is the specific entropy. Γ is always above unity for ideal gases, in which case $\Gamma = (\gamma + 1)/2$, where γ is the specific heat ratio. Thermodynamic regions exist in the vapor phase where $\Gamma < 1$, thus the speed of sound increases as the density decreases along an isentropic process, contrarily to the ideal-gas behavior. Therefore, both Z and Γ can be taken as a measure of the flow non-ideality. The trends of figure 1b clarify that, the nozzle is initially fed at non-ideal total conditions, then the ideal-gas state is monotonically approached as the test proceeds. The time signals for test M1.5 exhibit very similar trends and are therefore not discussed here.

4.2. Nozzle expansion

Nozzle expansions at different time and non-ideal conditions (Z_T), are analysed here for the considered tests. Instants of interest are selected in order to clearly distinguish among different levels of non-ideality during the run; therefore, five significant values of Z_T are selected in the minimum to maximum interval, namely $Z_T \in [0.82, 0.97]$ for test M2.0 and $Z_T \in [0.81, 0.98]$ for test M1.5. For all conditions the flow at the centerline is assumed to be isentropic.

For each test, figure 2 reports on the top a sketch of the planar nozzle profiles in non-dimensional coordinates, including the pressure taps where static pressure is measured (active taps). 8 out of 9 taps were active for test M2.0, while 4 taps, in the region of higher gradients, were available for test M1.5. x is the axial coordinate and the normalization factor is the nozzle semi-height H at the geometrical throat, which is located at $x/H = 10.29$. The sketches are superimposed to the schlieren images of the MDM vapor flow acquired at $t = 0$ s.

The schlieren image of test M2.0 shows the complex flow structure originated by the recessed step machined at the throat. A first expansion fan (dark region at $x/H \simeq 10.29$) rotates the flow at the step edge. An oblique shock (thin dark line) forms at the reattachment point, downstream a local separation, and a second fan (dark region at $x/H \simeq 10.80$) finally rotates the flow where the step plateau connects with the contoured profile. Shock waves are correctly visualized, while expansions (expected as bright regions) are not, due to an overstep of the measuring range related to the high compressibility of the MDM vapor flow. Further details can be found in [16,17]. Also, multiple shock reflections on the profiled walls are clearly visible, as well as weak waves generated by contoured wall roughness. The slope of such waves relative to the flow direction, whose analysis is underway for the two nozzles, represents a measure of the local Mach number. The oblique shock waves arising from the step perturb only locally the flow; moreover, though well visible in the schlieren images, shocks originate at low Mach number, $M \simeq 1.2$, and are therefore weak enough to cause a negligible reduction in total pressure (entropy production) as it has been proved, for the same geometry, in [18]. Hence, the flow can be assumed isentropic at the nozzle axis and the total pressure P_T is constant for the whole nozzle at a given time. The flow is also isentropic at the centerline of nozzle M1.5, which features a clean geometry and an increased roughness at the profile surface. The resulting Mach waves are therefore well visible in the divergent portion of the nozzle. The outlet section is also included in the optical domain; the nozzle operates in under-expanded conditions, as proven by the well visible expansion fans and the slip lines at the exit.

In the central portion of figure 2, the measured values of the static-to-total pressure ratio P/P_T are reported along the nozzle axis for active taps. These data are overlapped to the ones (almost continuous) extracted from a two-dimensional (2D) CFD viscous calculation performed using the SU2 solver and MDM vapor modeled as a polytropic ideal gas (MDM$_{PIG}$). The ideal specific heat ratio in the temperature range of interest is $\gamma = 1.018$. For nozzle M2.0 only, experimental results previously obtained [22] for the same nozzle operated with air are also plotted. The bottom part of figure 2 reports the compressibility factors Z along the axis, which are computed as a function of the measured static pressure P and of the specific entropy $s = s(P_T, T_T)$ upstream of the nozzle. The calculated Z are also reported for MDM$_{PIG}$ and for air (nozzle M2.0), with the rather obvious result of unity values.

A first comparison is made between the expansion line of MDM$_{PIG}$ and of air in terms of local pressure ratio P/P_T, which is always higher for MDM due to its higher molecular complexity and the consequent lower value of the specific heat ratio γ with respect to air ($\gamma_{air} = 1.4$). This is consistent with the prediction made by the simple one-dimensional
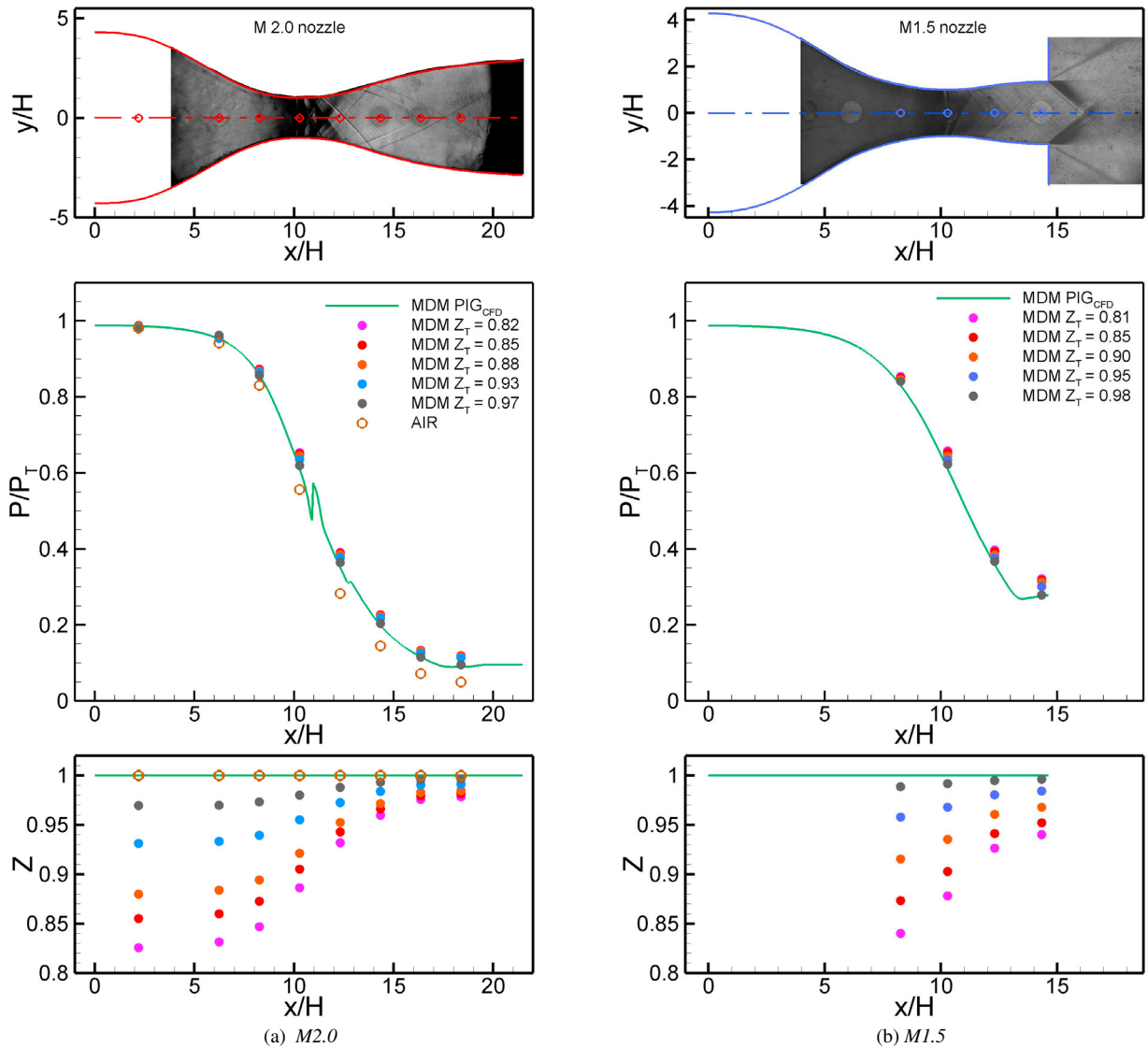
Fig. 2. Experimental results for test M2.0 (a) and M1.5 (b). Schlieren images (top) of the MDM vapor flow at time $t = 0$ s, overlapped to the nozzle non-dimensional geometries. Throat is located at $x/H = 10.29$. Experimental values at the axis of P/P_T (center) and calculated Z (bottom) as a function of the non-dimensional spatial coordinate x/H at different Z_T. CFD data from viscous calculation coupled with PIG model for MDM are superimposed to the experimental ones. For test M2.0 experimental points for the nozzle operated with air are also included.

theory for isentropic flows of perfect gases. Also, for a given nozzle geometry, the pressure ratio is found to be independent of the inlet total conditions. More interestingly the MDM$_{PIG}$ expansion line can be compared with the experimental data for MDM, thus putting in evidence non-ideal flow effects. For both nozzles, the local pressure ratio P/P_T is higher then the ideal-gas one and results to be dependent on the inlet conditions, thus confirming the non-ideal character of the flow. This behavior is well visible as the expansion proceeds along the nozzle and compressibility effects increase. The departure from the calculated ideal-gas behavior is higher at lower value of Z_T at inlet and reduces as dilute gas conditions are approached. This dependence is found to be not negligible even at the moderate non-ideal states explored. For instance, at the throat and for minimum Z_T, P/P_T values deviate of 7.2% (test M2.0) and 7.6% (M1.5) from their perfect-gas counterpart, and of 5.5% (M2.0) and 6.7% (M1.5) from the values measured at maximum Z_T. This effect is expected to increase at higher non-ideal conditions.

The departure of the measured data from the ideal gas behavior, with values of P/P_T increasing as higher non-ideal conditions are approached is qualitatively consistent with the prediction (not reported here) made by one-dimensional
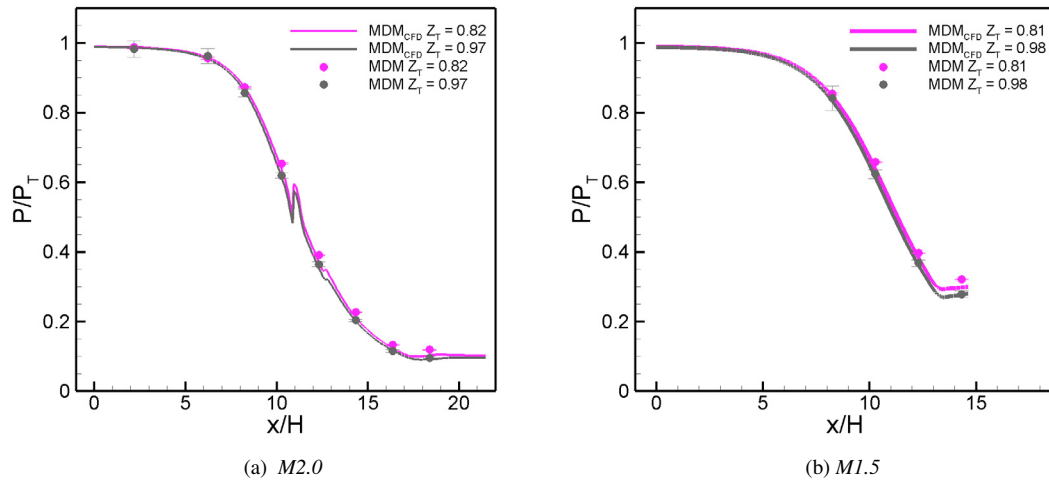
(a) *M2.0*　　　　　　　　　　　　　　　　　　(b) *M1.5*

Fig. 3. Comparison between experimental and CFD values of P/P_T at the nozzle axis as a function of x/H for test M2.0 and for test M1.5.

theory for isentropic flows implementing the polytropic van der Waals model, which is the simplest one taking into account inter-molecular forces which are responsible of non-ideal gas effects. A comparison of the experimental data with results of a simplified model based on the corresponding state principle is currently underway.

Here, an analysis of the non-ideal effects on nozzle expanding flows of MDM vapor is carried out referring to the local pressure ratio P/P_T along the nozzle axis, since only measured data are involved. Other properties, which are relevant for an accurate modelling of the flow, are influenced by non-ideal effects; these properties are calculated but not extensively reported. However they have a significant impact on the nozzle flow; for instance (concerning quantities involved in the mass flow calculation) at the throat of nozzle M2.0 and at the minimum Z_T, the PIG model underestimates the density of $\sim 20\%$, overestimates the speed of sound of $\sim 13\%$ and the Mach number of $\sim 4\%$.

Finally, figure 3 reports a comparison between the measured data and the ones extracted at the axis line from a 2D viscous CFD calculation, performed using the SU2 software suite coupled with the improved Peng-Robinson Stryjek-Vera (iPRSV) equation of state, exhibiting comparable accuracy with SW model in the explored region. For plot clarity, only data corresponding to maximum and minimum Z_T are reported. Uncertainty bars are also shown to indicate the accuracy of the measurements. For the two nozzles, the computed local pressure ratio P/P_T is in very good agreement with the measured one, except for the exhaust section, probably due to boundary-layer effects not properly caught by the 2D simulation. Also, the calculation is capable to correctly catch the effect and the position of the shock waves originated at the recessed step and of their reflection, as proven by the two bumps at $x/H \simeq 11$ and $x/H \simeq 12.7$, consistently with the schlieren image. Further details on the simulation can be found in [16].

5. Conclusion

The results of an extensive experimental campaign, aiming at studying compressible flows of molecularly complex vapors of interest for ORC power systems, are presented here for the first time. The fluid under scrutiny is the Siloxane MDM which is of interest due to its wide application in ORCs and to its high molecular complexity.

Experimental data are provided for nozzle expansions, which are fundamental flows in the field of NICFD and are typical in ORC turbine channels. Up to date, these data were lacking in the open literature, despite they are crucial to verify the accuracy of tools employed to model such unconventional flows.

The flow within two planar, converging-diverging nozzles has been investigated in terms of total pressure and temperature, of pressure field at the nozzle axis and of two-dimensional schlieren visualization. Inlet conditions ranged from moderate non-ideal states to the ideal-gas state, covering a thermodynamic region of application for ORC expanders. As expected, the vapor behavior reveals non-ideal, since the inlet condition significantly influence the expanding flow, in contrast to the perfect gas case. This proves that accounting for non-ideal effects is key in the

process of designing and the analyzing the performance of ORC turbo-expanders. In this perspective, the accurate predictions of the flow field provided by SU2 suite simulations is also proven.

The nozzle flow field is discussed here in terms of local pressure ratio P/P_T along the nozzle axis and of schlieren imaging. Further analysis will be presented relative to the evaluation of the local Mach number from schlieren images and to the assessment of simplified models to predict the thermodynamic behavior of ORC expansions.Tests at higher non-ideal conditions (closer to the critical point) are underway, and full results will be available in the near future.

Acknowledgements

References

[1] Colonna, P., Casati, E., Trapp, C., Mathijssen, T., Larjola, J., Turunen-Saaresti, T., et al. Organic rankine cycle power systems: From the concept to current technology, applications, and an outlook to thr future. ASME Journal of Engineering for Gas Turbines and Power 2015;137:100801–1–19.

[2] Macchi, E., Astolfi, M.. Organic Rankine Cycle (ORC) Power Systems. Technologies and applications. New York: Woodhead Publishing Series in Energy: Number 107, Elsevier; 2017.

[3] Vitale, S., Gori, G., Pini, M., Guardone, A., Economon, T.D., Palacios, F., et al. Extension of the su2 open source cfd code to the simulation of turbulent flows of fuids modelled with complex thermophysical laws. In: 22nd AIAA Computational Fluid Dynamics Conference. AIAA Paper 2760; 2015,.

[4] Pini, M., Persico, G., Pasquale, D., Rebay, S.. Adjoint method for shape optimization in real-gas flow applications. Journal of Engineering for Gas Turbines and Power 2015;137(3).

[5] Persico, G., Pini, M., Dossena, V., Gaetani, P.. Aerodynamics of Centrifugal Turbine Cascades. ASME J Eng Gas Turb Power 2015;137(112602):1–11.

[6] Span, R., Wagner, W.. Equations of state for technical applications. i. simultaneously optimized functional forms for nonpolar and polar fluids. International Journal of Thermophysics 2003;24(1):1–39.

[7] Colonna, P., van der Stelt, T.P.. FluidProp: a program for the estimation of thermo physical properties of fluids. Software, http://www.FluidProp.com; 2004. URL: www.FluidProp.com.

[8] Pini, M., Spinelli, A., Persico, G., Rebay, S.. Consistent look-up table interpolation method for real-gas flow simulations. Computers and Fluids 2015;107:178–188.

[9] Spinelli, A., Pini, M., Dossena, V., Gaetani, P., Casella, F.. Design, simulation, and construction of a test rig for organic vapours. ASME Journal of Engineering for Gas Turbines and Power 2013;135:042303.

[10] Pini, M., Spinelli, A., Dossena, V., Gaetani, P., Casella, F.. Dynamic simulation of a test rig for organic vapours. In: Proceedings of 5th Conference on Energy Sustainability, ASME EsFuelCell2011, Washington, Washington DC, USA. 2011,.

[11] Spinelli, A., Dossena, V., Gaetani, P., Osnaghi, C., Colombo, D.. Design of a test rig for organic vapours. In: Proceedings of ASME Turbo Expo, Glasgow, UK. 2010,.

[12] Colonna, P., Guardone, A.. Molecular interpretation of nonclassical gasdynamics of dense vapors under the van der Waals model. Phys Fluids 2006;18(5):056101–1–14.

[13] Guardone, A., Spinelli, A., Dossena, V.. Influence of molecular complexity on nozzle design for an organic vapor wind tunnel. ASME Journal of Engineering for Gas Turbines and Power 2013;135:042307.

[14] Palacios, F., Colonno, M.R., Aranake, A.C., Campos, A., Copeland, S.R., Economon, T.D., et al. Stanford University Unstructured (SU^2): An open-source integrated computational environment for multi-physics simulation and design. AIAA Paper 2013-0287 2013;51st AIAA Aerospace Sciences Meeting and Exhibit.

[15] Vimercati, D., Gori, G., Spinelli, A., Guardone, A.. Non-ideal effects on the typical trailing edge shock pattern of ORC turbine blades. In: 4th International Seminar on ORC Power Systems. 2017,.

[16] Gori, G., Zocca, M., Cammi, G., Spinelli, A., Guardone, A.. Experimental assessment of the open-source SU2 CFD suite for ORC applications. In: 4th International Seminar on ORC Power Systems. 2017,.

[17] Spinelli, A., Cozzi, F., Dossena, V., Gaetani, P., Zocca, M., Guardone, A.. Experimental investigation of a non-ideal expansion flow of siloxane vapor mdm. In: Proceedings of ASME Turbo Expo, Seoul, South Korea; vol. 3. 2016,.

[18] Cozzi, F., Spinelli, A., Carmine, M., Cheli, R., Zocca, M., Guardone, A.. Evidence of complex flow structures in a converging-diverging nozzle caused by a recessed step at the nozzle throat. In: 45th AIAA Fluid Dynamics Conference, Dallas, TX, USA, 22-26 June. 2015,.

[19] Antonini, C., Persico, G., Rowe, A.L.. Prediction of the dynamic respinde of complex transmission line system for unsteady pressure measurement. Measurement Science and Technology October 13, 2008;19(12).

[20] Hung, P.C., Irwin, G., Kee, R., McLoone, S.. Difference equation approach to two-thermocouples sensor characterization in constant velocity flow environment. Review of Scientific Instruments 2005;76(024902).

[21] Thompson, P.A.. A fundamental derivative in gas dynamics. Phys Fluids 1971;14(9):1843–1849.

[22] Spinelli, A., Guardone, A., Cozzi, F., Carmine, , Cheli, R., Zocca, M., et al. Experimental Observation of Non-ideal Nozzle Flow of Siloxane Vapor MDM. In: 3th International Seminar on ORC Power Systems. 103; 2015,.